The Journal of Neuroscience, May 1992, 12(5): 1789–1801

Multiple Ca^{2+} Currents Elicited by Action Potential Waveforms in Acutely Isolated Adult Rat Dorsal Root Ganglion Neurons

Reese S. Scroggs and Aaron P. Fox

Department of Pharmacological and Physiological Sciences, The University of Chicago, Chicago, Illinois 60637

Ca^{2+} entry into different diameter cell bodies of dorsal root ganglion (DRG) neurons depolarized with action potential (AP) waveform commands was studied using the whole-cell patch-clamp technique and pharmacological probes. We have previously shown that Ca^{2+} current expression in DRG neuron cell bodies depends on cell diameter. In small diameter DRG neurons, L- and N-type Ca^{2+} currents usually accounted for most Ca^{2+} entry during APs as determined by blockade with nimodipine and ω-conotoxin GVIA (ω-CgTx). In medium- diameter DRG neurons, T-type Ca^{2+} currents accounted for 29% or 54% of Ca^{2+} entry in cells held at −60 mV or −80 mV, respectively, based on blockade by amiloride. T-type Ca^{2+} currents did not usually contribute to Ca^{2+} entry in large diameter DRG neurons. An amiloride/ω-CgTx/nimodipine-resistant Ca^{2+} current was prominent in medium diameter DRG neurons, while L- and N-type Ca^{2+} currents played a relatively small role in Ca^{2+} entry. In all DRG neuron sizes, AP-generated currents were large in amplitude, resulting in significant Ca^{2+} entry. APs with slower rates of repolarization increased Ca^{2+} entry. In DRG neurons that expressed T-type Ca^{2+} currents, the duration of Ca^{2+} current entry during APs was prolonged, and this prolongation was reduced by amiloride. Thus, antagonists selective for different Ca^{2+} channels produced different patterns of blockade of AP-generated Ca^{2+} entry in different diameter DRG cell bodies. Selective Ca^{2+} channel modulation by neurotransmitters might be expected to have similar effects.

The main goal of the present study was to examine the relative contribution to Ca^{2+} entry into dorsal root ganglion (DRG) neurons during action potentials made by different Ca^{2+} channels. We have previously observed marked variation in Ca^{2+} current subtype expression between small (20–27 μm), medium (33–38 μm), and large (45–51 μm) diameter DRG neuron cell bodies (neurons), which may subserve different sensory modalities (Harper and Lawson, 1985a). In these previous studies, traditional rectangular depolarizing commands and 2 mM Ba^{2+} as the charge carrier were used (Scroggs and Fox, 1991, 1992). Under these conditions, T-type Ca^{2+} current was most prominent in medium diameter DRG neurons, L-type Ca^{2+} current was most prominent in small diameter DRG neurons, while N-type Ca^{2+} current contributed a similar amount to peak current in small, medium, and large diameter DRG neurons. A Ca^{2+} current that was not T-type Ca^{2+} current and was not sensitive to blockade by nimodipine or ω-conotoxin GVIA (ω-CgTx), and thus did not appear to be L-, or N-type Ca^{2+} current, was observed. This current was more prominent in large and medium diameter rat DRG neurons than in small diameter DRG neurons (Scroggs and Fox, 1992).

In the present study, action potential waveforms, recorded in current clamp from rat DRG neurons, were used as depolarizing stimuli to evoke Ca^{2+} currents in DRG neurons using the whole-cell patch-clamp technique (see McCobb and Beam, 1991). The resulting whole-cell Ca^{2+} currents were separated into components using pharmacological methods. Current through L-type Ca^{2+} channels was inhibited with the dihydropyridine (DHP) antagonist nimodipine (Fox et al., 1987a,b; Aosaki and Kasai, 1989). N-type Ca^{2+} channel currents were inhibited by ω-CgTx (McCleskey et al., 1987; Asoaki and Kasai, 1989; Plummer et al., 1989). T-type Ca^{2+} channels, which are relatively resistant to block by ω-CgTx or DHP antagonists (Fox et al., 1987a,b; McCleskey et al., 1987), were selectively blocked by amiloride (Tang et al., 1988; Scroggs and Fox, 1992).

The Ca^{2+} currents evoked by an action potential waveform (action potential command) in adult DRG neurons were of surprisingly large amplitude and somewhat resembled tail currents following the repolarization phase of a depolarizing rectangular command. As expected, T-type Ca^{2+} currents accounted for a large portion of the Ca^{2+} entering most medium diameter DRG neurons, contributed a smaller but significant amount to Ca^{2+} entry in some small diameter DRG neurons, and usually did not appear to be involved in Ca^{2+} entry in large diameter DRG neurons. L-type Ca^{2+} currents were observed to contribute more to Ca^{2+} entry in small diameter DRG neurons than in medium diameter DRG neurons. Also, the previously described non-T-type, nimodipine/ω-CgTx–insensitive Ca^{2+} current was responsible for a larger portion of the Ca^{2+} entry in medium diameter DRG neurons than in small diameter DRG neurons.

Surprisingly, T-type Ca^{2+} currents prolonged current entry, when present. In medium diameter neurons, changing the holding potential (HP) from −60 mV to −80 mV preferentially increased Ca^{2+} entry via T-type Ca^{2+} currents. Action potential commands with different shapes evoked different amounts of Ca^{2+} entry but did not alter the ratio of T-type Ca^{2+} current to high-threshold Ca^{2+} current.

The use of 2 mM Ca^{2+} as the charge carrier instead of 2 mM Ba^{2+} (used in our previous study, Scroggs and Fox, 1992) produced a shift in the current–voltage relationships probably due

Received Aug. 9, 1991; revised Dec. 10, 1991; accepted Dec. 18, 1991.

This work was supported by NIH and American Heart Association of Chicago awards to A.P.F. and NIH Award T32 HL 7237-15 to R.S.S.

Correspondence should be addressed to Reese S. Scroggs, Department of Pharmacological and Physiological Sciences, The University of Chicago, 947 East 58th Street, Chicago, IL 60637.

to a change in surface potential. This resulted in a positive shift in the potential where peak Ca^{2+} current occurred and increased the ratio of N- to L-type Ca^{2+} current in small diameter DRG neurons. In DRG neurons that expressed significant T-type Ca^{2+} currents, replacement of external Ba^{2+} with Ca^{2+} increased the ratio of T-type Ca^{2+} currents to high-threshold Ca^{2+} currents at HP −60 mV. Thus, Ca^{2+} entry via different Ca^{2+} channels during action potentials was often not predicted by previous whole-cell patch methods using standard rectangular commands to depolarize cells (Scroggs and Fox, 1991, 1992).

Materials and Methods

Acutely isolated cell bodies from dorsal root ganglia (DRG), lacking visible processes, were prepared from adult male rats, 200–250 gm (Harlan Sprague–Dawley) as previously described (Scroggs and Fox, 1991, 1992). Cell bodies (neurons) of three different diameter ranges were used in the present experiments; small (19–26 μm), medium (33–37 μm), and large (42–50 μm). Diameter was defined as the average of the distance along the longest and shortest axis of each cell body.

In most experiments, the depolarizing stimuli were scaled action potential waveforms (action potential commands) previously recorded from rat DRG neurons in current clamp. For comparative purposes, the same action potential waveform (illustrated in Fig. 2*A*) was usually used to evoke Ca^{2+} currents in different DRG neurons. In some experiments, action potential waveforms of different shape (Fig. 2*A–C*) were used to evoke Ca^{2+} currents in individual DRG neurons. The action potential commands were played back in the same time scale as they were recorded in order to allow a realistic assessment of Ca^{2+} entry. The recorded action potential commands were scaled to form voltage commands with holding potentials of −60 mV or −80 mV and a peak potential of +20 mV. For leak subtraction of capacitive currents and leakage currents, the cells were depolarized by an action potential command 1/10 original size. During data analysis, leak data were scaled and subtracted from the raw data.

The electrodes were coated with Sylgard and were heat polished to a resistance of 0.9–1.3 MΩ. Gigaohm seals were obtained in Tyrode's solution. Series resistance was compensated. In most cells included in the data analysis (12 large, 19 medium, and 17 small diameter DRG neurons) the capacitance time constant was estimated before and after series resistance compensation, from a capacity transient generated during a 10 mV hyperpolarization of the membrane potential. A curve-fitting program was used to find the best-fit single exponential function for the decay of the capacity transient. Membrane capacitance was measured by integrating the area under the capacity transient before series resistance compensation. Prior to recording of capacity transients for the purpose of calculating series resistance, the filter setting was temporarily changed from the usual 3 kHz to 20 kHz in order to prevent attenuation of the capacity transient. Series resistance was calculated before and after compensation using the formula

$$\text{series resistance} = \frac{\text{(capacitance time constant)}}{\text{(membrane capacitance)}}.$$

In a few cells (1 large, 5 medium, and 1 small), the capacity transient, after compensation, was too fast or noisy to allow accurate estimation of the capacitance time constant using the computer curve-fitting program. In these cells, the series resistance, which had been previously recorded from the series resistance compensation pot on the Axopatch

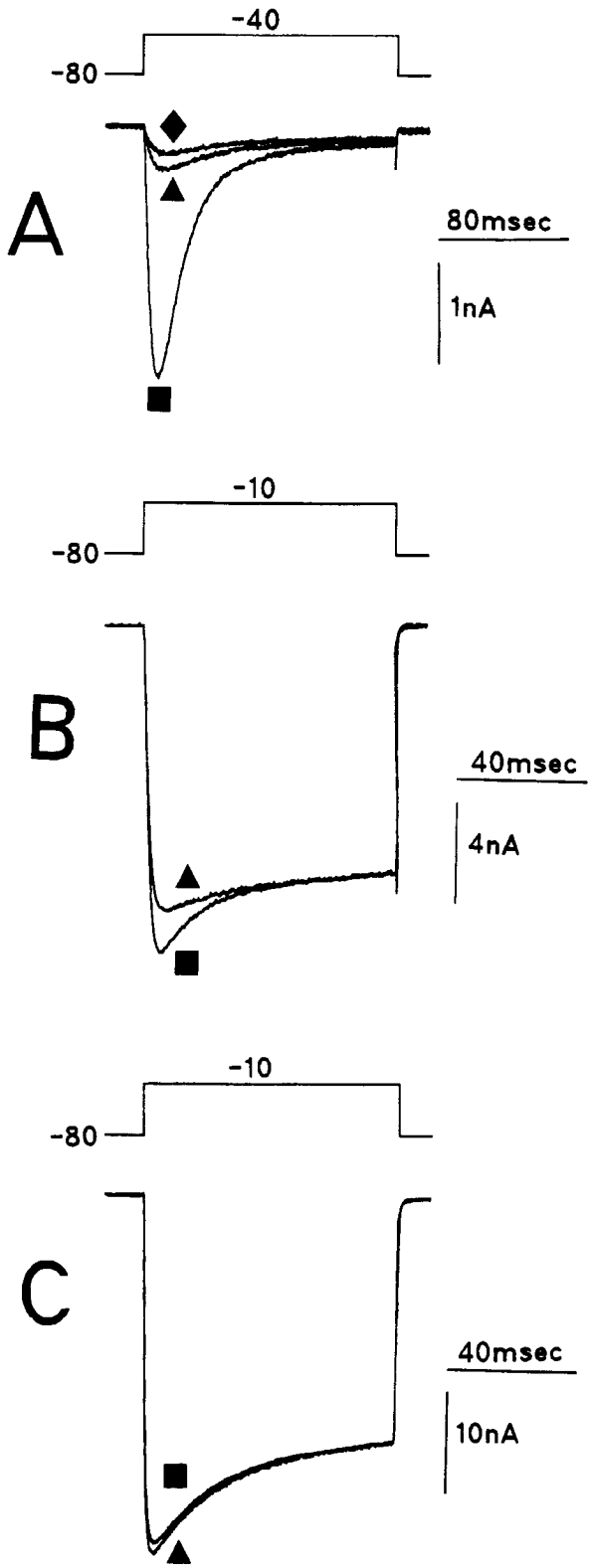

→

Figure 1. Amiloride selectively blocks T-type Ca^{2+} currents. *A*, T-type Ca^{2+} currents (■) were evoked in a medium diameter DRG neuron using a rectangular voltage step from HP −80 mV to −40 mV. Superfusion of the neuron with 500 μM amiloride blocked 83% of the T-type Ca^{2+} current (▲). Amiloride at 1000 mM blocked 90% of the T-type Ca^{2+} current (◆). *B*, High-threshold Ca^{2+} currents were evoked in the same neuron illustrated in *A* by using a test depolarization to −10 mV. Amiloride at 500 μM blocked 13% of peak current (▲) compared to control (■), but had no effect on steady state current. *C*, Amiloride at 500 μM (▲) did not block control high-threshold current (■) elicited in a large diameter DRG neuron that had no T-type Ca^{2+} currents. Holding potential was −80 mV and the test depolarization was to −10 mV. External solution (*A–C*) contained (in mM) 160 TEA-Cl, 2 $BaCl_2$, 10 HEPES, and 100 nM TTX, adjusted to pH 7.4 with TEA-OH. The pipette solution contained (in mM) 120 CsCl, 5 Na_2-ATP, 0.4 Na_2-GTP, 10 EGTA, and 20 HEPES, adjusted to pH 7.4 with CsOH. Series resistance after compensation was 0.49 MΩ in *A* and *B* and 0.17 MΩ in *C*.

1C, was subtracted from the series resistance calculated from a capacity transient recorded before compensation. Series resistance compensation ranged from 46% to 95% (average ± SEM, 79 ± 1.6%; $N = 55$), resulting in final series resistance values ranging from 1.65 MΩ to 0.09 MΩ (average ± SEM, 0.45 ± 0.05 MΩ; $N = 55$). In general, larger-tipped, lower-resistance electrodes were used on the larger cells (which expressed larger currents) in order to start out with lower series resistance and a rapidly settling clamp. No data were included in the analysis where series resistance resulted in a 10 mV or greater error in voltage commands.

To isolate Ca^{2+} currents in rat DRG neurons, the following solutions were employed. The internal solution contained 120 mM CsCl, 5 mM Na_2-ATP, 0.4 mM Na_2-GTP, 10 mM EGTA, and 20 mM HEPES, adjusted to pH 7.4 with CsOH (303 mOsm). For most experiments, the external solution contained 160 mM tetraethylammonium (TEA)Cl, 10 mM HEPES, 2 mM $CaCl_2$, and 100 nM tetrodotoxin, adjusted to pH 7.4 with TEA-OH (316 mOsm). For some experiments, 2 mM $CaCl_2$ was replaced by 2 mM $BaCl_2$.

T-type Ca^{2+} current was defined as rapidly inactivating, low-threshold current evoked from holding potentials of −60 mV to −90 mV using test depolarizations to −30 mV or −40 mV. T-type Ca^{2+} current was also defined by its sensitivity to blockade by amiloride. A stock solution of 500 mM amiloride was made by dissolving amiloride hydrochloride (Sigma) in dimethyl sulfoxide (DMSO). The stock solution was diluted to a concentration of 500 μM in the external buffer. The DMSO concentration for these experiments was 0.1%, which was previously determined to have no effect on T-type Ca^{2+} currents (Scroggs and Fox, 1992). The effects of amiloride at a concentration of 500 μM was specific for T-type Ca^{2+} currents. Figure 1*A* illustrates the effects of 500 μM and 1000 μM amiloride on a T-type Ca^{2+} current (2 mM Ba^{2+} as the charge carrier) evoked from a medium diameter DRG neuron using HP −80 mV and a test depolarization to −40 mV. The 500 μM concentration blocked 83% of the total inward current, while 1000 μM blocked 90%. Previous studies by us have determined that 500 μM amiloride blocked an average of 79% of T-type calcium current in medium diameter DRG neurons (Scroggs and Fox, 1992). Figure 1*B* illustrates the effects of 500 μM amiloride on peak Ca^{2+} current recorded from the same cell under the same conditions except that the test depolarization was to −10 mV, and other Ca^{2+} channels were activated. Only a relatively small portion of the peak current (which could be explained by blockade of T-type Ca^{2+} channels) was affected by the amiloride, while the steady state current was unchanged. Similar effects of 500 μM amiloride were observed on peak current in three additional medium diameter DRG neurons that expressed large T-type Ca^{2+} currents. In cells that had no T-type Ca^{2+} currents, amiloride was shown to have no effect on peak current. Figure 1*C* shows an experiment in which a large diameter neuron, lacking T-type Ca^{2+} currents, did not respond to amiloride. Thus, amiloride at a concentration of 500 μM does not appear to block high-threshold currents (Scroggs and Fox, 1992).

L-type Ca^{2+} current was defined as the current component blocked by the L-type Ca^{2+} channel antagonist nimodipine (Scroggs and Fox, 1991, 1992). N-type Ca^{2+} current was defined as the current component that was sensitive to blockade by the N-type Ca^{2+} channel antagonist ω-CgTx (Scroggs and Fox, 1991, 1992). In experiments where both were used, nimodipine was always applied first and then ω-CgTx was applied.

For all experiments the neurons were depolarized every 10 sec. The blocking effects of antagonists on calcium entry were determined from plots of picocoulombs of calcium entry versus time. In order to adjust for rundown, a straight line was drawn through the data points and extrapolated out over the earliest point where the slope of the calcium entry versus time relationship in the presence of antagonist matched that observed in the predrug control data. This point was regarded as the control calcium entry level. Because some rundown had possibly occurred between the apparent peak effect of the first antagonist and the addition of a second antagonist, the data regarding the second antagonist were adjusted by multiplying the percentage of the original calcium entry remaining at peak effect of the first antagonist by the percentage change produced by the second antagonist. This adjustment relies on the assumption that different channel subtypes remaining after treatment with the first antagonist run down at the same rate, and thus the second antagonist would have had the same relative effect if added closer in time to the peak effect of the first antagonist.

The statistical significance of differences between two means was made using the Student's *t* test. In some cases, where data were collected before and after treatment in the same neurons, a paired sample test was used (Zar, 1984).

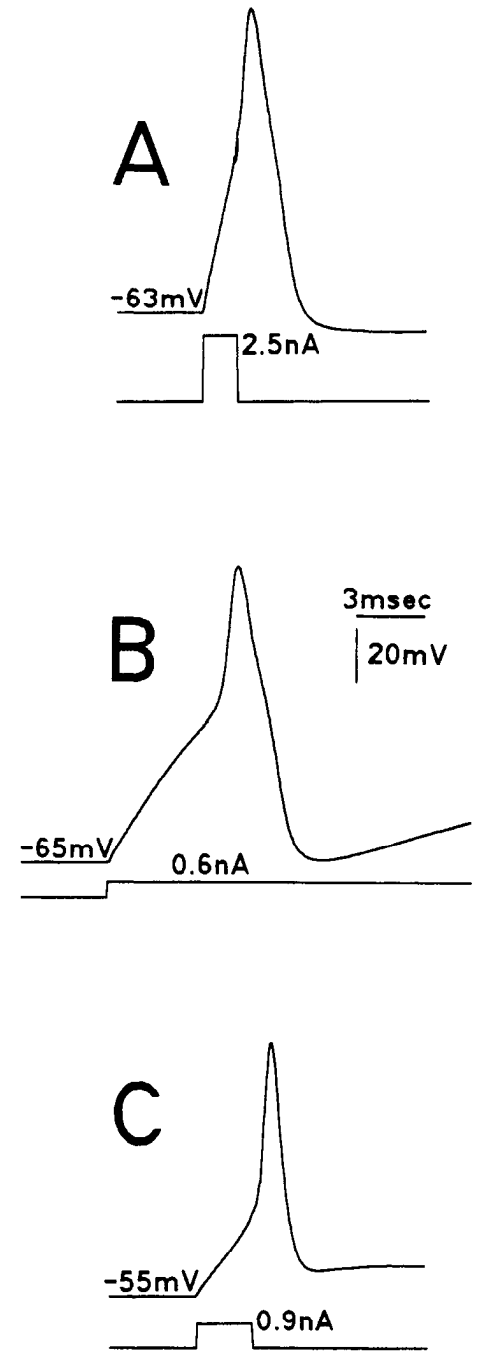

Figure 2. Action potentials recorded from different rat DRG neurons in current clamp. *A,* Action potentials were evoked from a medium diameter DRG neuron by a 1.5-msec-long injection of 2.5 nA of depolarizing current. The membrane potential was set to −63 mV by injecting 0.1 nA of hyperpolarizing current through the recording electrode. *B,* Action potentials were evoked from a small diameter DRG neuron by injection of 0.6 nA of depolarizing current for a duration of 23 msec. Resting membrane potential was −65 mV. *C,* Action potentials were evoked from a medium diameter DRG neuron by injection of 0.9 nA of depolarizing current for 2.4 msec. The membrane potential was set to −55 mV by 0.2 nA of hyperpolarizing current. In *A–C* the external solution was Tyrode's containing (in mM) 140 NaCl, 4 KCl, 2 $MgCl_2$, 2 $CaCl_2$, 10 glucose, and 10 HEPES, adjusted to pH 7.4 with NaOH. The pipette solution contained (in mM) 120 KCl, 5 Na_2-ATP, 0.4 Na_2-GTP, 10 EGTA, and 20 HEPES, adjusted to pH 7.4 with KOH. Calibration applies to *A–C.*

Results

Action potential waveforms

Illustrated in Figure 2 are three different action potentials recorded under current-clamp conditions from rat DRG neurons, elicited by slightly different methods of current injection. Figure 2*A* illustrates an action potential recorded from a medium diameter DRG neuron. The action potential was evoked with a large brief depolarizing current pulse in order to achieve a fast rate of rise on the ascending limb of the action potential. This fast rate of rise resembles that observed when action potentials are generated in DRG neurons via stimulation of the peripheral axon (Scroggs and Anderson, 1989). Based on the lack of an afterdepolarization (White et al., 1989), this medium diameter DRG neuron did not appear to express the large amplitude T-type Ca^{2+} currents usually observed in medium diameter DRG neurons (Scroggs and Fox, 1992). Figure 2*B* illustrates an action potential recorded from a small diameter DRG neuron that was depolarized by a small long-duration current pulse, resulting in a slow rate of rise. The action potential illustrated in Figure 2*C* was recorded from a medium diameter DRG neuron using an intermediate-intensity and -duration current injection, resulting in an intermediate rate of rise. This cell exhibited an afterdepolarization that was probably due to Ca^{2+} entry through T-type Ca^{2+} channels. In medium diameter DRG neurons that exhibited large T-type Ca^{2+} currents, an afterdepolarization following action potentials was always observed. These afterdepolarizations appeared at membrane potentials above −50 mV, increased in size following hyperpolarization of the membrane potential, and were nearly completely blocked by 500 μM amiloride. Except for activation at more depolarized membrane potentials, these afterdepolarizations resembled those previously described by White et al. (1989). Although the three action potential shapes illustrated here represent only some of the various action potential shapes observed in DRG neurons (Harper et al., 1985b), they had some interesting differences, and thus were used as voltage commands for the patch-clamp experiments (see Materials and Methods).

Small diameter DRG neurons

General characteristics. Ca^{2+} entry into small diameter (19–27 μm) DRG neurons was studied using a conventional step depolarization (rectangular command) and/or an action potential waveform command (action potential command), with 2 mM Ca^{2+} as the charge carrier. Figure 3*A* shows a family of currents elicited by rectangular command depolarizations from HP −60 mV. The maximal current was elicited by a depolarization to +10 mV. The average maximal current elicited by a rectangular command depolarization was 5.5 ± 0.86 nA (±SEM; HP −60 mV; $N = 17$). In general, the test potential at which the maximal current occurred varied from 0 to +10 mV, which was about a 10 mV shift in the positive direction from previous results with 2 mM Ba^{2+} as the charge carrier (Scroggs and Fox, 1991, 1992). In 16 small diameter DRG neurons, Ca^{2+} entry was also studied using an action potential command that depolarized the cells to +20 mV from HP −60 mV. The resulting current appeared quite different to that generated in response to a rectangular wave command (Fig. 3*B*). The amplitude of the action potential generated current averaged 5.9 ± 0.86 nA and had a duration of 1.74 ± 0.07 msec at $¼V_{max}$ ($N = 16$) ($¼V_{max}$ refers to a horizontal line through the current at one-fourth of the distance between zero current and the maximum current). The charge entering the cells averaged 8.2 $coul^{-12}$ ± 1.2 or 3.6 $coul^{-15}/\mu m^2$ membrane surface area (surface area estimated from capacitance measurements).

T-type Ca^{2+} currents. Most small diameter DRG neurons did not express significant T-type Ca^{2+} currents when depolarized with a rectangular command from HP −60 mV (see Fig. 3*A*). In 17 small diameter DRG neurons depolarized to −40 mV from HP −60 mV, low-threshold Ca^{2+} current averaged only 81 ± 16.5 pA. In three neurons where little T-type Ca^{2+} current was detected with rectangular command depolarizations, 500 μM amiloride failed to have any effect on action potential generated current as well (Fig. 3*B*). However, T-type Ca^{2+} currents were occasionally observed to play a role in Ca^{2+} entry in small diameter DRG neurons held at −60 mV. Figure 3*C* illustrates T-type Ca^{2+} currents evoked using rectangular commands to −30 mV from HP −80 mV and −60 mV. In this neuron, amiloride (500 μM) blocked 27% of the Ca^{2+} entry evoked by an action potential command from HP −60 mV (Fig. 3*D*). In five small diameter DRG neurons, 500 μM amiloride decreased action potential elicited Ca^{2+} entry by 8.8 ± 6.3%. A previous study demonstrated that 500 μM amiloride blocked only 79% of total T-type Ca^{2+} current (Scroggs and Fox, 1992). Thus, an average 8.8% block by amiloride is probably an underestimate. After correcting for incomplete block, we estimate that an average of 11.2% of the Ca^{2+} influx in small diameter neurons may have been via T-type Ca^{2+} channels.

High-threshold Ca^{2+} currents. Nimodipine and ω-CgTx were tested for their ability to block current generated by action potential commands in 10 small diameter DRG neurons held at −60 mV. Figure 4*A* illustrates the effects of nimodipine and ω-CgTx on charge entry over time in one such neuron. Previously, it was determined that this cell did not express T-type Ca^{2+} current at HP −60 mV. Superfusion with 2 μM nimodipine blocked 37% of the Ca^{2+} entering the neuron. Subsequent application of 0.9 μM ω-CgTx blocked another 42% of Ca^{2+} entering the neuron, leaving 21% of the Ca^{2+} entry unblocked. Figure 4*B* illustrates the currents from this experiment under control conditions and after blockade by nimodipine and ω-CgTx. On average, Ca^{2+} entry was decreased by an average of 27 ± 5.4% by 2 μM nimodipine ($N = 10$). Seven of the neurons were subsequently treated with 0.9 μM ω-CgTx, which resulted in the rapid blockade of another 50 ± 10.0% of the original control Ca^{2+} entry. In six neurons treated with both nimodipine and ω-CgTx, and which had previously been determined not to express detectable T-type Ca^{2+} current, an average of 25 ± 6.6% of the original control Ca^{2+} entry was insensitive to blockade by the combination of the two antagonists. Figure 4*C* illustrates the nimodipine-sensitive current, the ω-CgTx–sensitive current, and the nimodipine/ω-CgTx–resistant current from the same neuron depicted in Figure 4, *A* and *B*.

Medium diameter DRG neurons

General characteristics. Figure 5*A* shows a family of currents elicited by rectangular command depolarizations from HP −60 mV, with 2 mM Ca^{2+} as the charge carrier. In seven medium diameter DRG neurons that were held at −60 mV and stimulated with a rectangular command, the maximal current averaged 6.8 ± 1.3 nA (Fig. 5*A*). Figure 5*B* shows currents elicited from HP −80 mV. From HP −80 mV, peak current averaged 9.2 ± 0.8 nA ($N = 10$). Figure 5, *C* and *D*, plots peak current as a function of voltage (*I–V*) at HP −60 mV (Fig. 5*C*) and HP −80 mV (Fig. 5*D*). Both *I–V* curves show a shoulder at negative

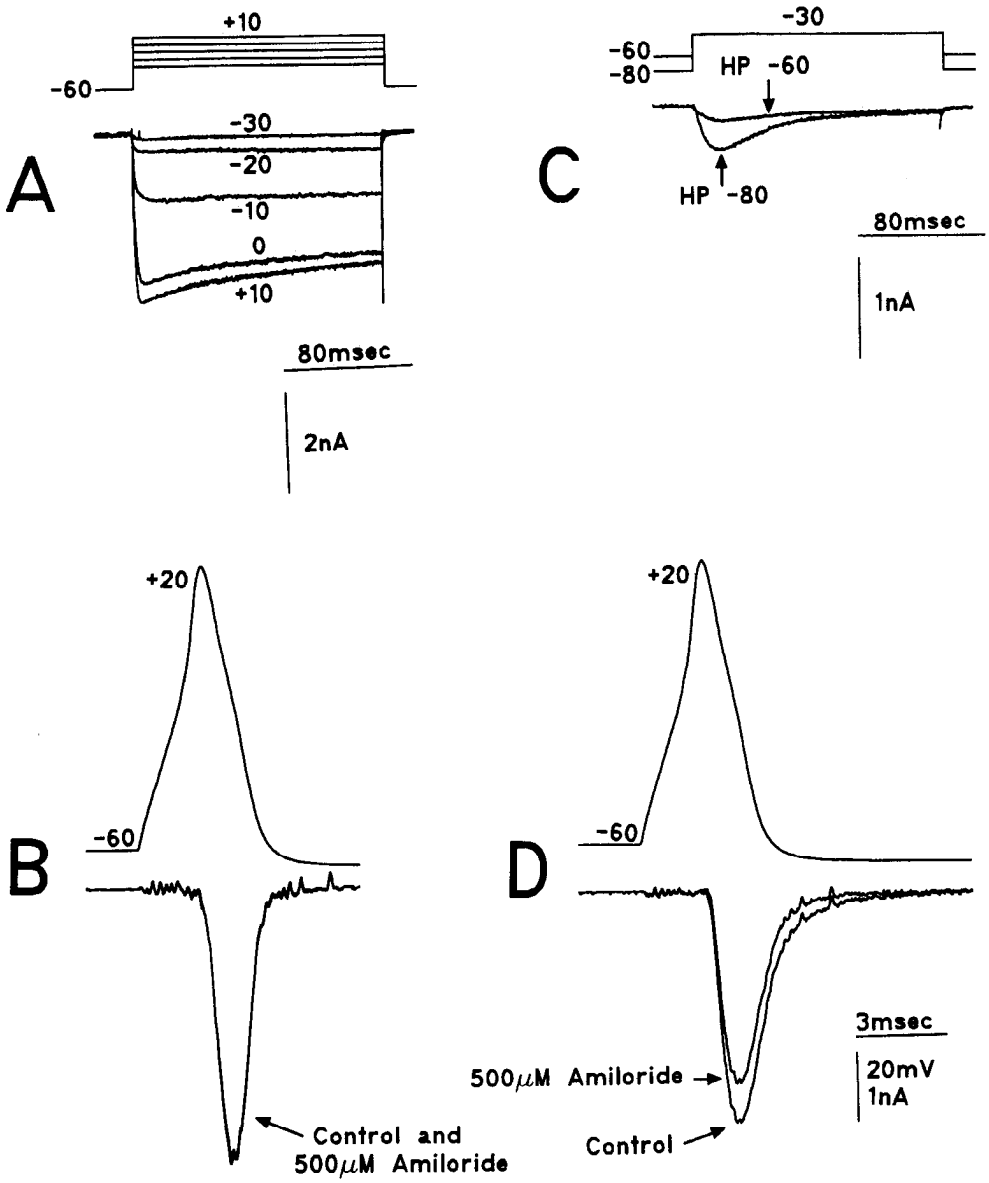

Figure 3. A comparison of Ca^{2+} currents elicited by action potential waveforms to those elicited by rectangular voltage steps. *A*, A family of Ca^{2+} currents was evoked from a small diameter DRG neuron by a rectangular voltage step from HP −60 mV to test potentials ranging from −30 mV to +10 mV, in a neuron showing no T-type Ca^{2+} current. *B*, A large inward Ca^{2+} current was generated in response to an action potential command from HP −60 mV to a peak potential of +20 mV in the same neuron shown in *A*. Superfusion of the neuron with 500 μM amiloride had no effect on the action potential generated current. *C*, T-type Ca^{2+} current evoked by a voltage step from a holding potential of −60 mV or −80 mV to a test potential of −30 mV, in a neuron that expressed T-type Ca^{2+} currents. *D*, A large inward Ca^{2+} current was evoked in response to an action potential command in the same neuron shown in *C*. Amiloride (500 μM) blocked 27% of the Ca^{2+} entering the neuron, much of which entered late in the sweep. Solutions in *A–D* were the same as those in Figure 1, except that 2 mM $CaCl_2$ replaced 2 mM $BaCl_2$ in the external solution. Series resistance after compensation was 0.4 MΩ in *A* and *B* and 0.88 MΩ in *C* and *D*. Calibration in *D* also applies to *B*.

potentials, due to activation of T-type Ca^{2+} currents (Fig. 5*C,D*). In addition, the currents were maximal near 0 mV, representing a 10 mV shift in the depolarizing direction when compared to previous experiments with 2 mM Ba^{2+} (Scroggs and Fox, 1992).

T-type Ca^{2+} currents. T-type Ca^{2+} currents were very prominent in medium diameter DRG neurons. Rectangular commands to −30 mV elicited T-type Ca^{2+} currents averaging 0.89 ± 0.16 nA in cells held at −60 mV (N = 10) and 4.0 ± 0.33 nA in cells held at −80 mV (N = 13). T-type Ca^{2+} current amplitude was roughly ninefold larger in medium than in small diameter DRG neurons, when compared under identical conditions ($p < 0.05$).

When medium diameter DRG neurons were stimulated with action potential commands, large inward currents were observed (Fig. 5*E,F*). The current averaged 9.7 ± 1.2 nA in amplitude, and 18.2 ± 3.55 $coul^{-12}$ of charge entered the cell per action potential (N = 7). Although the duration of the current at $¼V_{max}$ (2.87 ± 0.23 msec; N = 7) was significantly longer than that observed in small diameter DRG neurons under the same conditions ($p < 0.05$), the charge per square micron of membrane surface area in medium DRG neurons (3.1 ± 0.47 $coul^{-15}$; N = 7) was not significantly different from that observed in small diameter DRG neurons (p = 0.24). At HP −80 mV, the action potential generated current averaged 12.4 ± 1.12 nA in amplitude and had a duration of 3.32 ± 0.12 msec (N = 10) at $¼V_{max}$. An average of 31.8 ± 2.59 $coul^{-12}$ of Ca^{2+} entered the cells during each action potential (5.3 ± 0.30 $coul^{-15}$ $Ca^{2+}/\mu m^2$; N = 10).

A substantial fraction of Ca^{2+} influx during action potential commands occurred via T-type Ca^{2+} channels. In the neuron depicted in Figure 5*E*, which was held at −60 mV, amiloride blocked 19% of influx. In another medium diameter DRG neuron held at −80 mV (illustrated in Fig. 5*F*) amiloride blocked 60% of influx. Note that the amiloride preferentially inhibited the current occurring late in the depolarization, probably resulting from the slow activation and deactivation kinetics of T-type Ca^{2+} currents (discussed below). In five medium diameter DRG neurons held at −60 mV, amiloride (500 μM) decreased Ca^{2+} entry by 29.5 ± 3.3%. In eight different medium diameter DRG neurons held at −80 mV, the same concentration of ami-

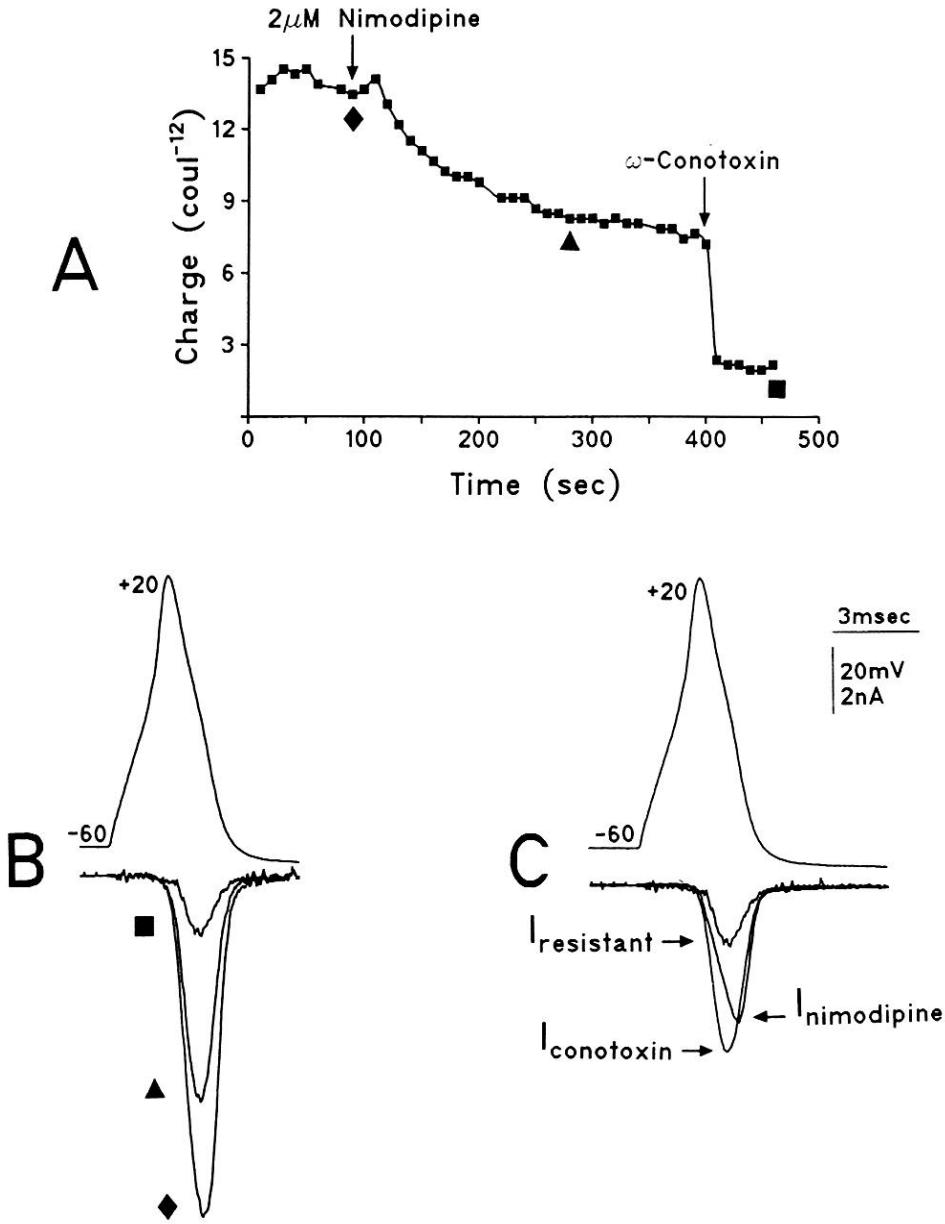

Figure 4. Effects of nimodipine and ω-CgTx on Ca^{2+} influx elicited by action potential commands in small diameter DRG neurons. *A*, Ca^{2+} influx was elicited using the template illustrated in *B*. Total charge entering the neuron was calculated by integrating the area under the current after leak subtraction. The neuron was depolarized every 20 sec. After a base line was established, the superfusion medium was switched to one containing 2 μM nimodipine (*first arrow*), which blocked 37% of the Ca^{2+} entering the neuron. After the effect of nimodipine stabilized, the neuron was exposed to 0.9 μM ω-CgTx (*second arrow*), which blocked another 42% of the Ca^{2+} influx, leaving 21% of the Ca^{2+} entering the neuron unblocked. *B*, Superimposed current traces that illustrate time points along the graph of charge entry versus time shown in *A*: ◆, control; ▲, after blockade by nimodipine; ■, after blockade by ω-CgTx. *C* shows nimodipine-sensitive Ca^{2+} current, ω-CgTx–sensitive Ca^{2+} current, and the Ca^{2+} current that was resistant to blockade by the two antagonists. The records for $I_{nimodipine}$ and $I_{\omega\text{-CgTx}}$ were obtained by computer subtraction. The solutions were the same as those in Figure 3. Series resistance after compensation was 0.49 MΩ. Calibration bar applies to *B* and *C*.

loride decreased Ca^{2+} entry by 54.1 ± 1.8%. Because previous studies have shown that 500 μM amiloride blocked only 79% of T-type Ca^{2+} current (Scroggs and Fox, 1992), we have corrected our data accordingly. Thus, we estimate that in medium diameter DRG neurons, T-type Ca^{2+} current may have made up as much 37.3% of the total action potential generated current at HP −60 mV and 68.5% of the total action potential generated current at HP −80 mV; values much larger than would be estimated using rectangular command depolarizations.

An additional study was performed to define more precisely the effect of holding potential on T-type Ca^{2+} current amplitude in medium diameter DRG neurons. Each cell in this study was initially held at −40 mV or −50 mV and the holding potential was increased in 5 mV or 10 mV increments to −90 mV or −95 mV (Fig. 6). The cells were held at each new potential until the amplitude of the T-type Ca^{2+} currents ceased increasing in amplitude. Figure 6*A* shows a family of T-type Ca^{2+} currents elicited by rectangular commands to −30 mV, from a variety of holding potentials. Figure 6*B* shows a plot of peak T-type Ca^{2+} current as a function of holding potential. A Boltzmann equation fitted to the data by eye yielded a $V_{½}$ of −68 mV (Fig. 6*B*). The threshold for T-type Ca^{2+} current repriming appeared to be about −50 mV.

High-threshold Ca^{2+} currents. Nimodipine (2 μM) and ω-CgTx (0.9 μM) were tested for their ability to block Ca^{2+} entering medium diameter DRG neurons in which large T-type Ca^{2+} currents had previously been observed. For these experiments, the cells were held at −60 mV and depolarized with an action potential command. Illustrated in Figure 7*A–D* is one of several cells where 500 μM amiloride, 2 μM nimodipine, and 0.9 μM ω-CgTx were all tested. On average, 3–6 min of superfusion with 2 μM nimodipine resulted in a decrease of 4.5 ± 3.2% (N = 6). Subsequent exposure of the neurons to 0.9 μM ω-CgTx resulted in a rapid blockade of 18.5 ± 2.8% of the original control Ca^{2+} influx, leaving 77% unblocked (N = 6). Approximately 37% (after correction for incomplete blockade of T-type Ca^{2+} currents

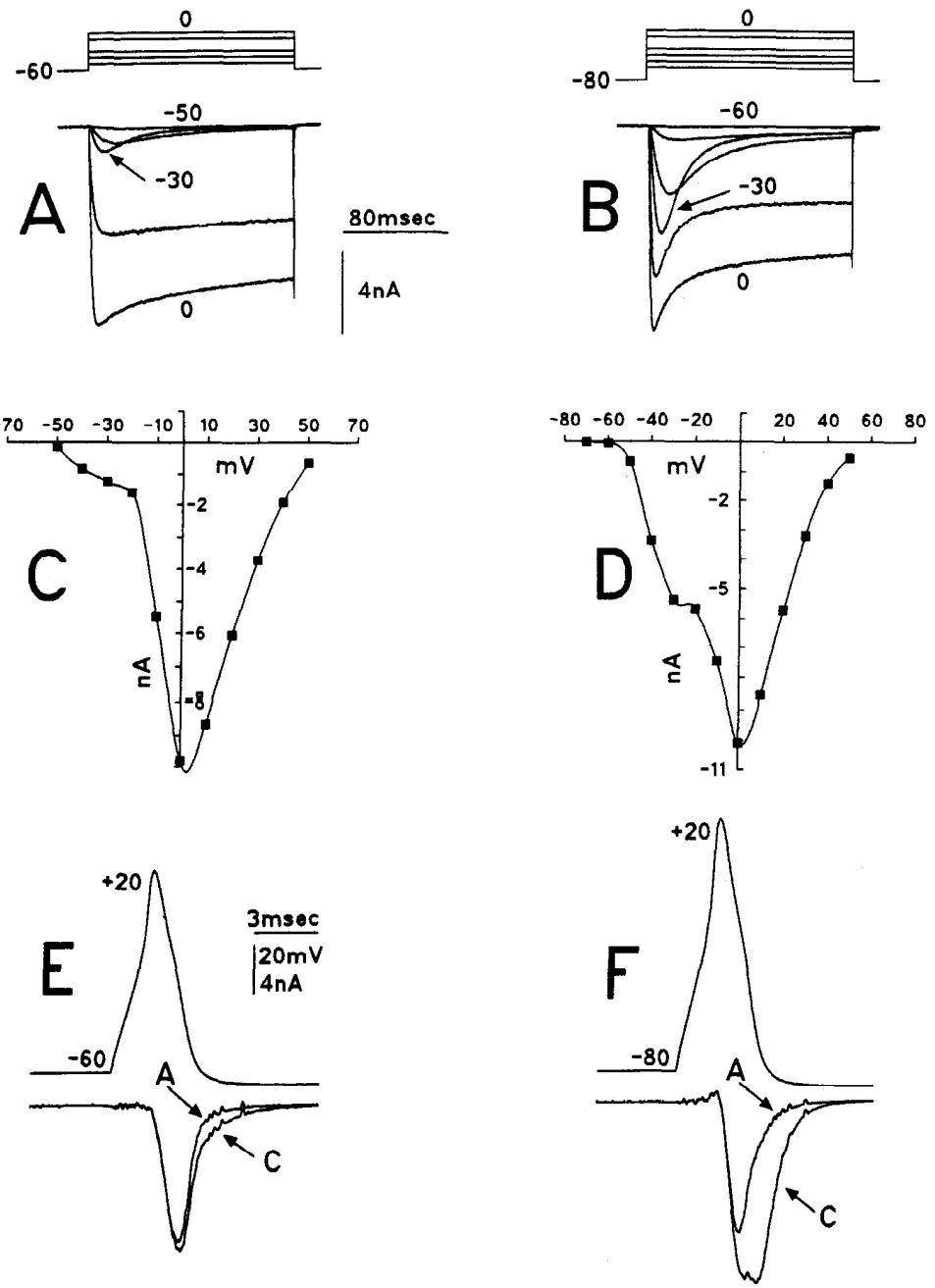

Figure 5. Large T-type Ca^{2+} currents were observed in medium diameter DRG neurons, using either step depolarizations or action potential templates. *A* and *B*, Families of Ca^{2+} currents evoked from two medium diameter DRG neurons held at −60 mV (*A*) and −80 mV (*B*) and depolarized to a variety of test potentials. *C* and *D*, Graphs of the *I–V* relationships observed in neurons depicted in *A* and *B*, respectively. Notice the shoulder on the ascending limb of the *I–V* curves produced by the activation of T-type Ca^{2+} currents. *E* and *F*, Superimposed action potential generated Ca^{2+} currents evoked from the neurons depicted in *A* and *B*, respectively, before (*C*) and after (*A*) superfusion of the neurons with 500 μM amiloride to block T-currents. The solutions were the same as those in Figure 3. Calibration in *A* applies to both *A* and *B*, and calibration in *E* applies to both *E* and *F*. Series resistance after compensation was 0.22 MΩ in *A*, *C*, and *E* and 0.3 MΩ in *B*, *D*, and *F*.

by 500 μM amiloride) of the Ca^{2+} influx could be accounted for by T-type Ca^{2+} channels (based on average blockade by amiloride in five of the neurons). Thus, approximately 40% of Ca^{2+} influx in medium diameter neurons was attributable to nimodipine/ω-CgTx–resistant high-threshold Ca^{2+} current. Figure 7, *B* and *C*, illustrates the action potential–generated currents before and after blockade by amiloride and ω-CgTx. Notice that the two antagonists block primarily different parts of the current, although there was some overlap. Figure 7*D* illustrates separately the amiloride-sensitive current, ω-CgTx–sensitive current, and the amiloride/nimodipine/ω-CgTx–resistant current in the neuron depicted in Figure 7*A–C*. The currents peaked at different times and most of the current was conducted through amiloride-sensitive and amiloride/nimodipine/ω-CgTx–resistant pathways. Note that up to 21% of the amiloride/nimodipine/ω-CgTx–resistant current illustrated in Figure 7*D* may be due to unblocked T-type Ca^{2+} current.

Large diameter DRG neurons

In contrast to medium diameter DRG neurons, T-type Ca^{2+} currents appear to play a minimal role in Ca^{2+} entry in most large diameter DRG neurons. Only 1 of 13 large diameter DRG neurons tested exhibited T-type Ca^{2+} current. Figure 8 shows data from a large diameter neuron that had no T-type Ca^{2+} currents. T-type Ca^{2+} currents were not observed in *I–V* plots (Fig. 8*A*) or in the current traces (Fig. 8*B*), even though the neurons were held at −80 mV. Peak Ca^{2+} current, which averaged 29 ± 3.0 nA (N = 13), occurred between −10 mV and 0 mV. This represented a shift of about 10 mV in the depolarizing direction compared to previous experiments with 2 mM Ba^{2+} as

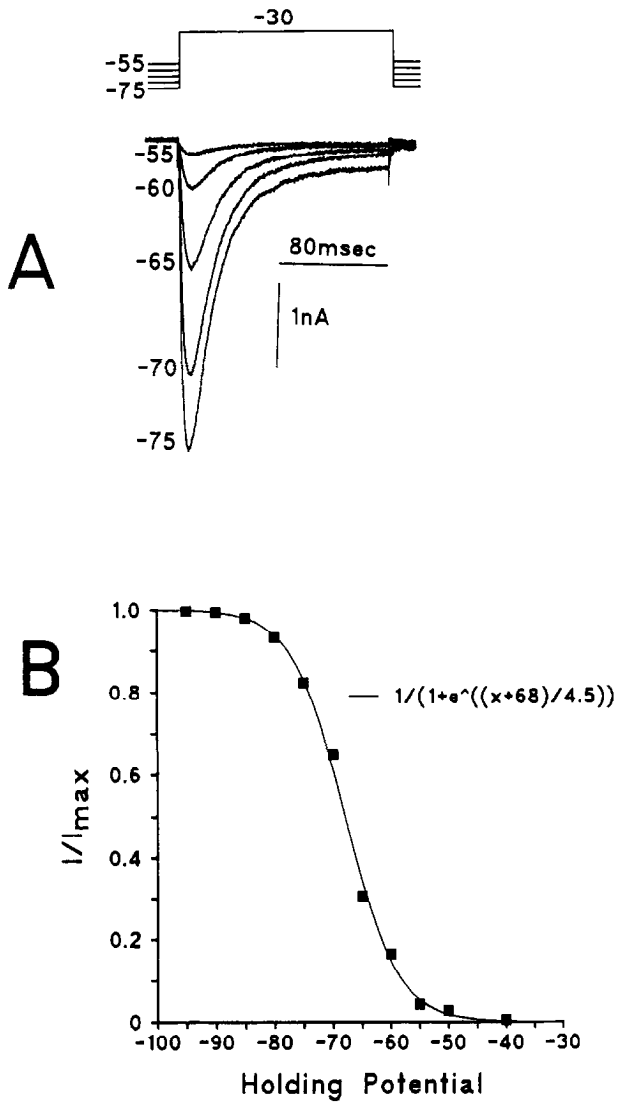

Figure 6. Effect of holding potential on T-type Ca^{2+} currents. *A* illustrates increase in the amplitude of T-type Ca^{2+} currents elicited in a medium diameter DRG neuron, as the holding potential was made more negative. Each holding potential was maintained until the T-type Ca^{2+} currents stabilized. For clarity, only those currents evoked from holding potentials ranging from −55 mV to −75 mV in 5 mV increments are included, although the entire range of holding potentials in this neuron was from −40 mV to −90 mV. *B* graphs Ca^{2+} current amplitude versus holding potential from medium diameter DRG neurons; each data point (■) represents the average of four to six neurons. In each neuron the holding potential was varied from −40 mV or −50 mV to −90 mV or −95 mV in 5 mV or 10 mV increments. The peak Ca^{2+} current amplitude was assigned the value of 1.0 and the rest of the currents were normalized to that value. The data from the experiment depicted in *A* are included in the graph. The data were fit by a Boltzmann relationship of the form $I/I_{max} = 1/[1 + \exp^{(V_{cell}+68)/4.5}]$. The solutions were the same as those in Figure 3. Series resistance after compensation ranged from 0.19 MΩ to 1.59 MΩ (average, 0.54 ± 0.24 MΩ; $N = 6$).

the charge carrier instead of 2 mM Ca^{2+} (Scroggs and Fox, 1992). Action potential–generated currents elicited from HP −80 mV in large diameter DRG neurons had surprisingly large amplitudes (39.7 ± 7.2 nA; $N = 9$), which resulted in an average of 45.9 ± 7.9 $coul^{-12}$ ($N = 9$) of Ca^{2+} entry per action potential. Although the duration of the action potential–generated currents in large diameter DRG neurons (1.52 ± 0.07 msec at $¼V_{max}$) was significantly less than the duration of currents evoked under identical conditions in medium diameter DRG neurons ($p < 0.05$), the Ca^{2+} entry per square micron of membrane surface area (4.4 ± 0.64 $coul^{-15}$) was not ($p = 0.14$). On average, amiloride (500 μM) had very little effect on Ca^{2+} entry during action potential commands (average decrease, 3.1 ± 3.4%; $p > 0.1$, paired-sample test). In the one large diameter cell that expressed T-type Ca^{2+} current, amiloride (500 μM) blocked 18% of the Ca^{2+} entering late in the action potential command depolarization.

Different action potential templates

The effects of different action potential shapes on Ca^{2+} entry were studied using the action potentials shown in Figure 2, *A–C*, after scaling. Variation in action potential command shape produced a significant difference in the total Ca^{2+} that entered the neurons. In six medium diameter DRG neurons held at −80 mV, action potential A (from Fig. 2*B*) elicited 38.7 ± 2.2 $coul^{-12}$ of influx; action potential B (from Fig. 2*A*) elicited 28.5 ± 1.4 $coul^{-12}$ of influx; action potential C (from Fig. 2*C*) elicited 16.7 ± 1.9 $coul^{-12}$ of influx. The peak average Ca^{2+} current amplitude evoked by action potentials A–C was 12.5 ± 0.6 nA, 11.8 ± 1.0 nA, and 9.5 ± 0.7 nA, respectively. Interestingly, the percentage of Ca^{2+} entry that was blocked by amiloride (500 μM) was virtually identical for all three action potential shapes. Amiloride blocked an average of 53.7 ± 2.4%, 53.0 ± 2.3%, and 55.0 ± 3.8% of the Ca^{2+} entry that was elicited by action potentials A–C, respectively.

As illustrated in Figure 9, *A–C*, Ca^{2+} current usually did not begin to flow until very near the peak of the action potential command was reached, regardless of shape. However, in two medium diameter DRG neurons depolarized with action potential A, which had the slowest rate of rise, a small amount of amiloride-sensitive Ca^{2+} current had begun to flow at the very beginning of the Ca^{2+} current trace. This may indicate that the stimulus provided by the slowly rising ascending limb of action potential A was close to threshold for T-type Ca^{2+} channels. Another interesting observation was that for each different action potential command, the current peaked well before the membrane potential had completely repolarized (Fig. 9*A–C*). There appeared to be a relationship between the rate of repolarization on the descending limb of the action potential command and the voltage at which peak current was observed. Average peak current was observed at around −31 mV for action potential A, which had the slowest rate of repolarization, −35 mV for action potential B, which had an intermediate rate of repolarization, and −39 mV for action potential C, which had the fastest rate of repolarization.

In large diameter DRG neurons, varying the shape of the action potential command had effects on current similar to that observed for medium diameter DRG neurons (Fig. 9*D–F*). In five large diameter neurons, action potential A stimulated entry of the most Ca^{2+} (71.5 ± 12.5 $coul^{-12}$) followed by action potential B (57.6 ± 10.0 $coul^{-12}$), and then action potential C (29.2 ± 6.6 $coul^{-12}$). The average peak current amplitudes evoked by action potentials A–C were 51.4 ± 8.4 nA, 50.6 ± 7.7 nA, and 45.6 ± 8.5 nA, respectively (Fig. 9*D–F*).

Calcium current did not begin to flow in large diameter DRG neurons until the peak potentials had been reached during each action potential command (Fig. 9*D–F*). The current peaked at different potentials on the descending limb of the different action potential commands, forming a pattern similar to that observed

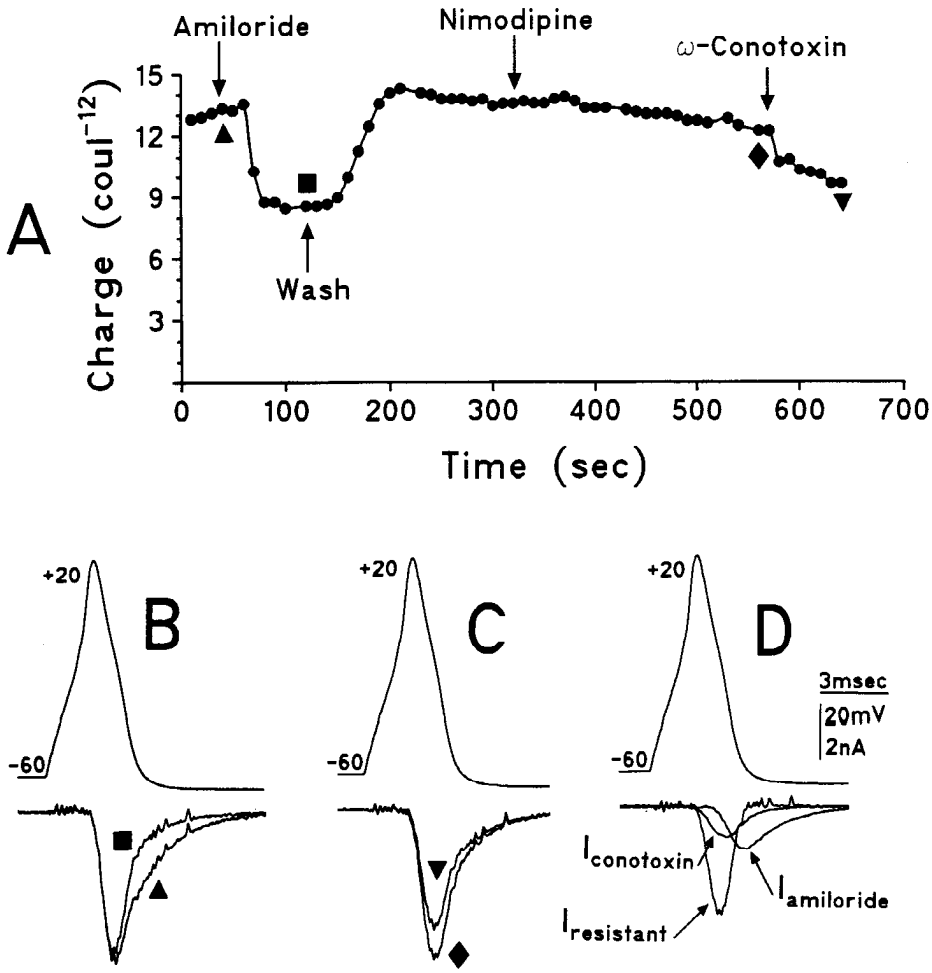

Figure 7. Effects of amiloride, nimodipine, and ω-CgTx on Ca^{2+} influx into a medium diameter DRG neuron. *A*, Control current elicited using the action potential command illustrated in *B*. Superfusion of the neuron with 500 μM amiloride (*first arrow*) blocked 35% of the Ca^{2+} entry, which was completely reversible upon washout of drug (*second arrow*). After a new base line was established, the superfusate was switched to one containing 2 μM nimodipine (*third arrow*), which had minimal effect on Ca^{2+} entry. Subsequent exposure of the neuron to 0.9 μM ω-CgTx (*fourth arrow*) blocked 18% of Ca^{2+} entry. *B*, Superimposed current traces that illustrate the effects of amiloride in the experiment depicted in *A*: ▲, control; ■, after blockade by 500 μM amiloride. *C*, Current traces illustrating the effects of ω-CgTx in the experiment depicted in *A*; ◆, control; ▼, after blockade by ω-CgTx. *D* shows amiloride-sensitive Ca^{2+} currents, ω-CgTx–sensitive Ca^{2+} currents, and the Ca^{2+} current that was resistant to blockade by amiloride, nimodipine, and ω-CgTx. The solutions were the same as those in Figure 3: Series resistance after compensation was 0.35 MΩ. Calibration applies to *B–D*.

in medium diameter DRG neurons. The current peaked at −25 mV, −37 mV, and −39 mV, when cells were depolarized with action potentials A–C, respectively.

Discussion

The data in this report illustrate the roles played by different Ca^{2+} channels in the entry of Ca^{2+} into different diameter DRG neurons during action potentials. In small diameter DRG neurons, nimodipine-sensitive and ω-CgTx–sensitive Ca^{2+} currents appeared to be important pathways for action potential stimulated Ca^{2+} entry at physiological holding potentials (~−60 mV). The amount of Ca^{2+} entry that was blocked by 2 μM nimodipine in small diameter cells (27%) during action potential command depolarizations was less than that observed in previous experiments (Scroggs and Fox, 1992) where 2 mM Ba^{2+} was the charge carrier and rectangular command depolarizations were used. In the previous Scroggs and Fox (1992) study, ~53% of peak current was inhibited by 2 μM nimodipine. In contrast, ω-CgTx blocked about 50% of action potential elicited Ca^{2+} entry in the present experiments but only about 30% of peak Ba^{2+} current was blocked by ω-CgTx when rectangular commands were used in the previous Scroggs and Fox (1992) study. In all of the above experiments, HP −60 mV was used.

Some of the discrepancies between the effects of nimodipine and ω-CgTx in the present study and those observed in the previous Scroggs and Fox (1992) study may be explained in part by an increase in polarization of the transmembrane potential produced by the use of 2 mM Ca^{2+} as the charge carrier in the present study, rather than 2 mM Ba^{2+} that was used in the previous study. Calcium has been hypothesized to neutralize negative surface charges on the outside of the cell membrane more potently than Ba^{2+}, which results in a greater voltage drop across the nerve cell membrane (Frankenhaeuser and Hodgkin, 1952; Ohmori and Yoshii, 1977; Hille, 1984). Thus, more N-type Ca^{2+} channels may be reprimed in the presence of $[Ca^{2+}]_o$ versus $[Ba^{2+}]_o$ at HP −60 mV whereas L-type Ca^{2+} channels would be almost completely reprimed in the presence of either $[Ca^{2+}]_o$ or $[Ba^{2+}]_o$ (Fox et al., 1987a,b). This would tend to increase the proportion of whole-cell Ca^{2+} current carried by ω-CgTx–sensitive N-type Ca^{2+} channels. An increase in membrane polarization due to the use of Ca^{2+} instead of Ba^{2+} may also explain the positive shift in the voltage at which peak currents were observed in the present study.

Another reason for the decrease in blockade by nimodipine may be due to the inverse relationship between DHP efficacy and membrane potential (Bean, 1984; Sanguinetti and Kass, 1984; Cohen and McCarthy, 1987). Substituting Ca^{2+} for Ba^{2+} might make nimodipine less effective due to an increase in transmembrane potential. However, a previous study by us in small diameter DRG neurons determined that changes in membrane potential from −60 mV to −80 mV produced changes in the blockade of whole-cell current by ω-CgTx and nimodipine that were similar to those seen in this study, but only about a

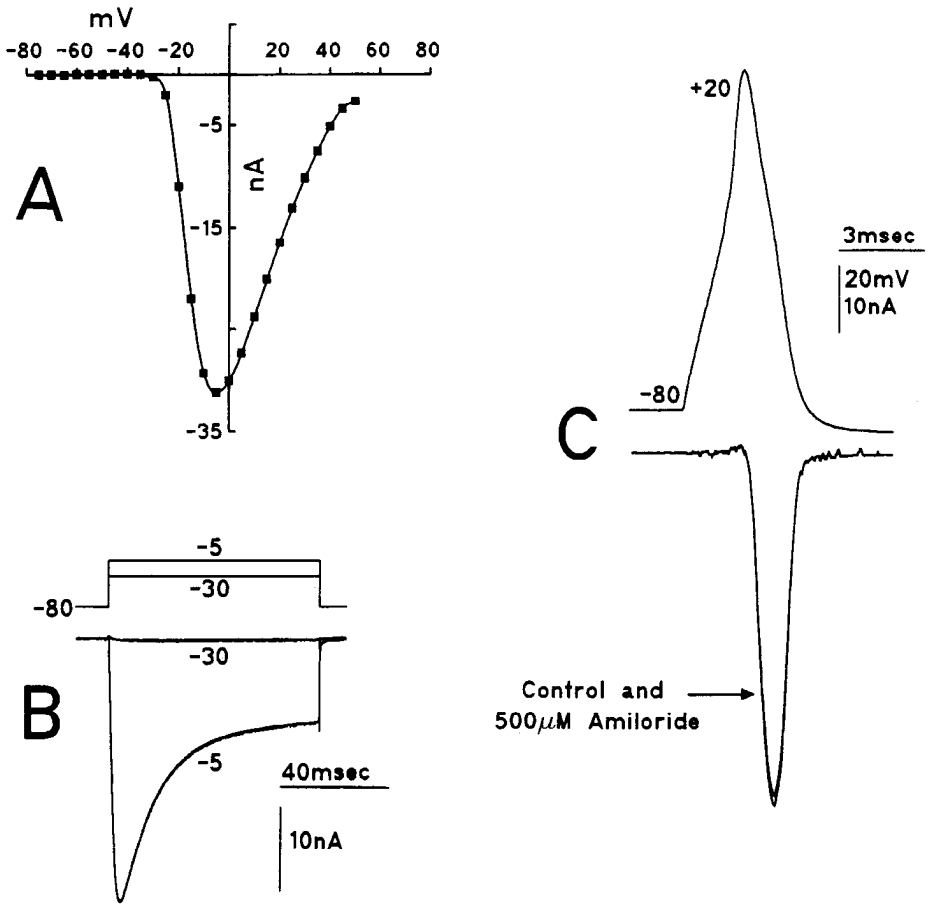

Figure 8. Lack of T-type Ca^{2+} currents in large diameter DRG neurons. *A*, *I–V* relationship in a large diameter DRG neuron. Notice the lack of a shoulder at negative potentials. *B*, Illustration of currents recorded from the same neuron depicted in *A*. Note that a test potential to −30 mV evoked very little current compared to the peak current that was observed upon depolarization to −5 mV. *C*, Superimposed traces illustrating the lack of effect of 500 μM amiloride on the action potential generated current in the same neuron depicted in *A* and *B*. The solutions were the same as those in Figure 3. Series resistance after compensation was 0.17 MΩ.

third of the decrease in nimodipine blockade could be attributed to a change in efficacy (Scroggs and Fox, 1991).

Other factors may be involved in the differences observed between action potential commands and rectangular command depolarizations. Action potential command currents somewhat resemble tail currents generated by the termination of a rectangular command. Also, the action potential commands were of short duration. Thus, the relative proportions of current conducted through the various Ca^{2+} channels may be strongly influenced by the activation and deactivation characteristics of the individual channels.

A significant amount (25%) of Ca^{2+} entry in small diameter DRG neurons during action potentials was observed to occur through a nimodipine/ω-CgTx–insensitive pathway similar to that (18%) observed using rectangular commands (Scroggs and Fox, 1992). Although some of the nimodipine/ω-CgTx–resistant current observed in this study may reflect L-channels that were not blocked by 2 μM nimodipine, previous studies indicate that there is a nimodipine/ω-CgTx–resistant Ca^{2+} current in rat DRG neurons (Scroggs and Fox, 1992). This current was not blocked by the presence of both 2 μM nimodipine and 5 μM ω-CgTx at a membrane potential of −40 mV (Scroggs and Fox, 1992). Nimodipine/ω-CgTx–resistant channels have also been demonstrated in other neuronal types such as cerebellar Purkinje cells, hippocampal CA3 neurons, and dorsal raphe neurons (Llinas et al., 1989; Mogul and Fox, 1991; Penington et al., 1991; Regan, 1991; Regan et al., 1991). In some small diameter DRG neurons, T-type Ca^{2+} current appeared to be a significant pathway for Ca^{2+} entry during action potentials as demonstrated by blockade of charge entry by the specific T-type Ca^{2+} channel blocker amiloride. Thus L-, N-, and T-type, as well as nimodipine/ω-CgTx–insensitive Ca^{2+} channels all appear to be involved in Ca^{2+} entry during action potentials in small diameter DRG neurons.

Several characteristics of Ca^{2+} entry into medium diameter DRG neurons were different than in small diameter DRG neurons. Although the amount of Ca^{2+} entering the cell per unit surface area was not different between the two size ranges, the average duration of the Ca^{2+} current elicited by an action potential command was nearly twice as long in medium diameter DRG neurons when compared to small diameter DRG neurons. This difference appeared to be mainly due to the expression of large T-type Ca^{2+} currents in medium diameter DRG neurons (see also McCobb and Beam, 1991). The data indicated that the Ca^{2+} entering medium diameter neurons late in the sweep was probably entering via T-type Ca^{2+} channels and is probably a result of the slow activation and deactivation properties of these channels (Fox et al., 1987a,b). The finding that large T-type Ca^{2+} currents were observed in medium diameter neurons in the present study agrees with a previous study where the average amplitude of T-type Ca^{2+} currents was largest in medium diameter DRG neurons (Scroggs and Fox, 1992).

We also studied the steady state inactivation properties of the T-type Ca^{2+} currents. The midpoint of the $H - \infty$ was at −68 mV ($V_{1/2}$), which is 10 mV more positive than that determined from a previous study (Fox et al., 1987a). The deviation cannot be accounted for by differences in external solution since the Fox et al. study used 10 mM Ca^{2+} as the charge carrier, which

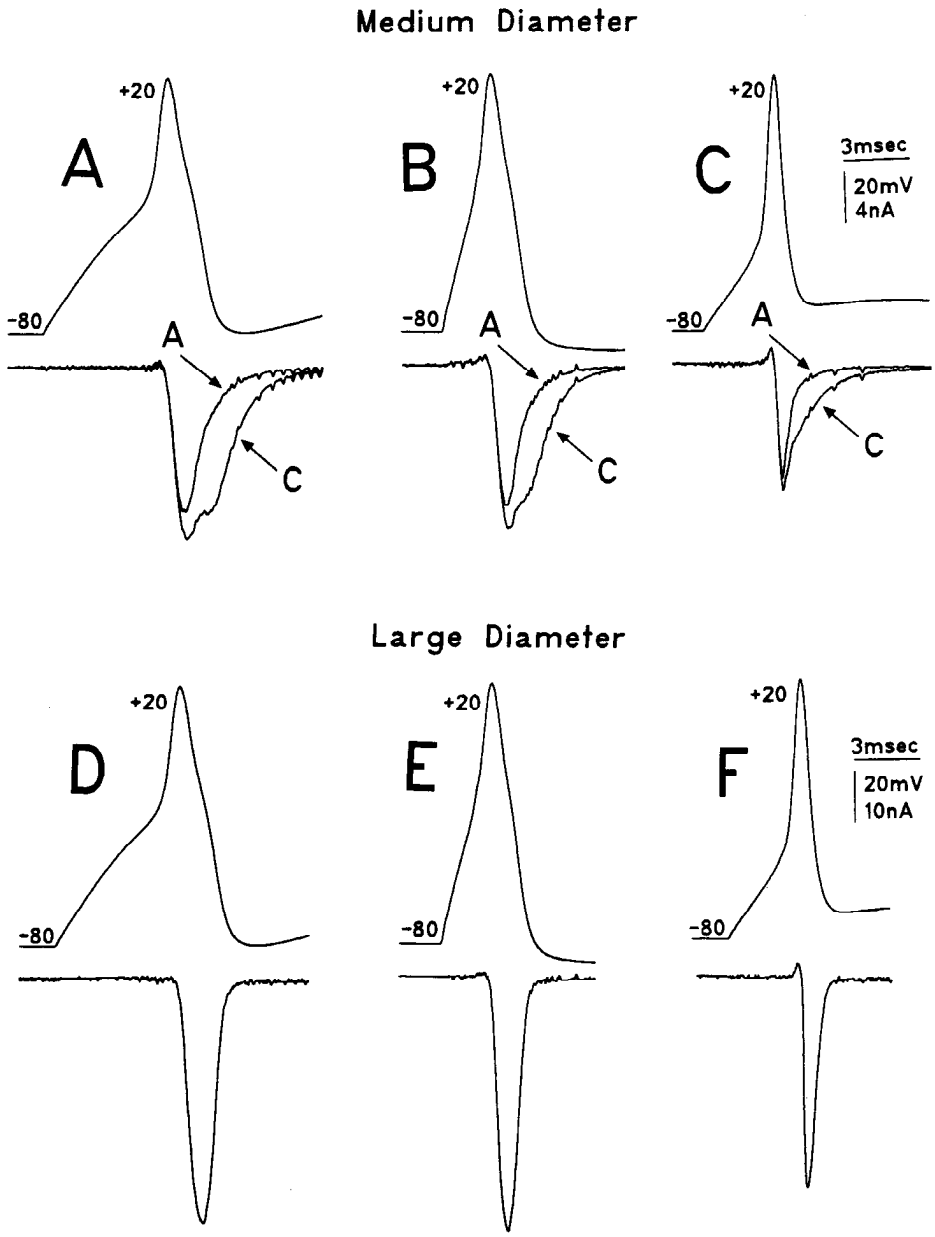

Figure 9. Ca^{2+} influx was altered by the use of different action potential shapes as the command potential. *A–C,* Superimposed currents recorded before and after superfusion with 500 μM amiloride using three different action potential commands, in a medium diameter neuron. Notice that while the total amount of charge that entered the neurons was altered by changes in the shape of the action potential, there was little change in the relative proportion of the current which was sensitive to block by 500 μM amiloride. *D–F,* Currents recorded from a large diameter DRG neuron using the same three action potential commands. The currents did not begin to flow until near peak depolarizing voltage had been reached, regardless of the rate of rise of the action potential command. The solutions were the same as those in Figure 3. Series resistance after compensation was 0.32 MΩ in *A–C* and 0.17 MΩ in *D–F.*

would shift the transmembrane potential in the wrong direction to explain the difference in V_{h}. However, the present study utilized a pipette solution that perfused the inside of the cells with 400 μM GTP, while the pipette solution in the Fox et al. (1987a) study lacked GTP. Thus, the difference may be due to T-channel sensitivity to some GTP-dependent activity. The difference may represent a species variation, as the previous study was performed on chick DRG neurons. Alternatively, the channels may have been altered in some way by the culture conditions used in the previous study. [We had previously reported that T-type Ca^{2+} currents were completely inactivated in medium diameter rat DRG neurons when 2 mM Ba^{2+} was the charge carrier, a conclusion based on depolarizing the cells to −50 mV from HP −60 mV (Scroggs and Fox, 1992). However, further analysis revealed that larger depolarizations from HP −60 mV did evoke a little T-type Ca^{2+} current in rat medium diameter DRG neurons when 2 mM Ba^{2+} was used as the charge carrier (R. S. Scroggs and A. P. Fox, unpublished observations).]

Very little nimodipine-sensitive Ca^{2+} current was involved in Ca^{2+} entry during action potentials in medium diameter DRG neurons, consistent with a previous study (Scroggs and Fox, 1992). Also, a significant amount (≈29%) of Ca^{2+} entry via high-threshold channels was blocked by exposure of the medium diameter DRG neurons to 0.9 μM ω-CgTx, a result similar to that obtained in a previous study using rectangular commands and 2 mM Ba^{2+} (Scroggs and Fox, 1992). Sixty-three percent of Ca^{2+} influx elicited by action potential commands at HP −60 mV was estimated to occur via nimodipine/ω-CgTx–resistant high-threshold Ca^{2+} channels in medium diameter DRG neurons, a result similar to data obtained previously using rectangular commands and 2 mM Ba^{2+} as the charge carrier (Scroggs and Fox, 1992). In the earlier study (Scroggs and Fox, 1992) the contribution to peak current amplitude made by T-type Ca^{2+} currents was small compared to the large amplitude of high-threshold Ba^{2+} currents.

In a previous study, large diameter DRG neurons were found

to be similar to medium diameter DRG neurons regarding the expression of nimodipine-sensitive, ω-CgTx–sensitive, and nimodipine/ω-CgTx–resistant Ca^{2+} currents (Scroggs and Fox, 1992). However, large diameter DRG neurons appear to be completely devoid of T-type Ca^{2+} currents (Scroggs and Fox, 1992). This observation was confirmed in the present study by showing that amiloride had no significant effect on Ca^{2+} entry in these cells. Because the large diameter DRG neurons had no significant T-type Ca^{2+} currents, the currents elicited by an action potential command were of much shorter duration than those observed in medium diameter DRG neurons. It is possible that the variation in the duration of Ca^{2+} entry has an effect on the nature of intracellular signaling. Interestingly, there was not a significant difference in Ca^{2+} entry per unit area of surface membrane between small, medium, and large diameter DRG neurons when stimulated by the same action potential command from HP −60 mV.

Differently shaped action potential commands resulted in significant variations in Ca^{2+} entry in medium and large diameter DRG neurons. The amount of Ca^{2+} entry may be correlated with the rate of repolarization of the action potential commands, with slower rates of depolarization facilitating Ca^{2+} entry. Although other dissimilarities existed between the three action potential templates employed in the present study, they do not appear to explain the differences in Ca^{2+} entry. The relative proportion of the current carried through T-type Ca^{2+} channels versus high-threshold Ca^{2+} channels appeared to be very stable. This result appears to be at odds with that of McCobb and Beam (1991), who reported that increasing the width of the action potential command preferentially increased high-threshold Ca^{2+} current versus T-type Ca^{2+} current. In the McCobb and Beam (1991) study, the action potential duration was increased by altering the rate of repolarization far beyond that which we observed to occur naturally in *medium* diameter DRG neurons. However, we have frequently recorded action potential durations in *small* diameter DRG neurons, which have greatly prolonged durations (Scroggs and Fox, unpublished observations). In these cells, which sometimes express T-type currents, the effects of prolonged action potential duration on the ratio of T-type Ca^{2+} current to high-threshold Ca^{2+} current may be significant.

Calcium influx did not begin until near the peak potential of the action potential command was reached, even though there was considerable variation in the rate of rise between the different commands. This pattern may be explained by the slow rate of activation of Ca^{2+} channels stimulated with small test depolarizations. However, in two cells depolarized with a slowly rising action potential command (action potential A), a small amount of amiloride-sensitive T-type Ca^{2+} current had begun to flow at the beginning of the current trace. This early amiloride-sensitive current has also been observed by McCobb and Beam (1991). The data may imply that for very fast rates of depolarization, the threshold for Na^{+} current activation will be reached before significant T-type Ca^{2+} current flow is initiated. At slower rates of depolarization, T-type Ca^{2+} currents may activate and facilitate spike generation as well as serve a possible role in intracellular Ca^{2+} signaling.

We observed that for each different action potential command, the current peaked well before the membrane potential had fallen to its lowest value. The rate of repolarization on the falling limb of the action potential command appeared to affect the voltage at which the current peaked, with slower rates resulting in a peak occurring at more positive potentials. At least two factors may have controlled the potential at which the peak current was observed; an increase in the driving force on Ca^{2+} ions, which becomes greater as the membrane potential becomes more negative, and a voltage-dependent deactivation of the Ca^{2+} channels, which becomes more rapid as the membrane potential becomes more negative. A slower rate of repolarization favors the deactivation of Ca^{2+} channels over the increase in current flow caused by the increased driving force, resulting in the occurrence of peak current at more depolarized potentials.

In conclusion, it appears that different Ca^{2+} currents participate in Ca^{2+} entry to various degrees during action potentials in DRG neurons of assorted diameters. It is possible that the variation in the duration of the action potential current elicited by the activation of different Ca^{2+} channels may serve an important role in intracellular Ca^{2+} signaling. Changes in membrane potential will significantly alter Ca^{2+} entry through the different Ca^{2+} channels. If the differences in Ca^{2+} channel expression exist in sensory neuron peripheral receptors and/or afferent terminals, as well as at the cell body, they may have significant effects on sensory transmission. Since DRG neurons with different diameter cell bodies may carry separate sensory information, selective modulation of certain Ca^{2+} channels may result in the independent modulation of specific sensory modalities.

References

Aosaki T, Kasai H (1989) Characterization of two kinds of high-voltage-activated Ca-channel currents in chick sensory neurons: differential sensitivity to dihydropyridines and ω-conotoxin GVIA. Pfluegers Arch 414:150–156.

Bean BP (1984) Nitrendipine block of cardiac calcium channels: high-affinity binding to the inactivated state. Proc Natl Acad Sci USA 81: 6388–6392.

Cohen CJ, McCarthy RT (1987) Nimodipine block of calcium channels in rat anterior pituitary cells. J Physiol (Lond) 387:195–225.

Fox AP, Nowycky MC, Tsien RW (1987a) Kinetic and pharmacological properties distinguish three types of calcium currents in chick sensory neurons. J Physiol (Lond) 394:149–172.

Fox AP, Nowycky MC, Tsien RW (1987b) Single channel recordings of three types of calcium channels in chick sensory neurons. J Physiol (Lond) 394:173–200.

Frankenhaeuser B, Hodgkin AL (1952) The action of calcium on the electrical properties of squid axons. J Physiol (Lond) 137:218–244.

Harper AA, Lawson SN (1985a) Conduction velocity is related to morphological cell type in rat dorsal root ganglion neurones. J Physiol (Lond) 359:31–46.

Harper AA, Lawson SN (1985b) Electrical properties of rat dorsal root ganglion neurones with different peripheral nerve conduction velocities. J Physiol (Lond) 359:47–63.

Hille B (1984) Ionic channels in excitable membranes, pp 426. Sunderland, MA: Sinauer.

Hirning LD, Fox AP, McCleskey EW, Miller RJ, Olivera BM, Thayer SA, Tsien RW (1988) Dominant role of N-type Ca^{2+} channels in evoked release of norepinephrine from sympathetic neurons. Science 239:57–61.

Llinas RR, Sugimori M, Cherksey B (1989) Voltage-dependent calcium conductances in mammalian neurons: the P channel. Ann NY Acad Sci 560:103–111.

McCleskey EW, Fox AP, Feldman D, Cruz LJ, Olivera BM, Tsien RW, Yoshikami D (1987) ω-Conotoxin: direct and persistent blockade of specific types of calcium channels in neurons but not muscle. Proc Natl Acad Sci USA 84:4327–4331.

McCobb DP, Beam KG (1991) Action potential waveform voltage-clamp commands reveal striking differences in calcium entry via low and high voltage-activated calcium channels. Neuron 7:119–127.

Mogul DJ, Fox AP (1991) Characterization of Ca channels in acutely isolated hippocampal CA3 pyramidal neurons: possible evidence for four different types of Ca channels. J Physiol (Lond) 433:259–281.

Ohmori H, Yoshii M (1977) Surface potential reflected in both gating and permeation mechanisms of sodium and calcium channels of the tunicate egg cell membrane. J Physiol (Lond) 267:429–463.

Penington NJ, Kelly JS, Fox AP (1991) A study of the mechanism of Ca^{2+} current inhibition produced by serotonin in rat dorsal raphe neurons. J Neurosci 11:3594–3609.

Plummer MR, Logothetis DE, Hess P (1989) Elementary properties and pharmacological sensitivies of calcium channels in mammalian peripheral neurons. Neuron 2:1453–1463.

Regan L, Sah DWY, Bean BP (1991) Ca^{2+} channels in rat central and peripheral neurons: high-threshold current resistant to dihydropyridine blockers and ω-conotoxin. Neuron 6:269–280.

Regan LJ (1991) Voltage-dependent calcium currents in Purkinje cells from rat cerebellar vermis. J Neurosci 11:2259–2269.

Sanguinetti MC, Kass RS (1984) Voltage-dependent block of calcium channel current in the calf cardiac Purkinje fiber by dihydropyridine derivatives. Circ Res 55:284–297.

Scroggs RS, Anderson EG (1989) Serotonin modulates a calcium-dependent plateau of action potentials recorded from bull frog A-type sensory neurons which is ω-conotoxin GVIA-sensitive, but dihydropyridine-insensitive. Brain Res 485:391–395.

Scroggs RS, Fox AP (1991) Distribution of dihydropyridine and ω-conotoxin-sensitive calcium currents in acutely isolated rat and frog sensory neuron somata: diameter dependent L channel expression in frog. J Neurosci 11:1334–1346.

Scroggs RS, Fox AP (1992) Calcium current variation between acutely isolated adult rat dorsal root ganglion neurons of different size. J Physiol (Lond) 445:639–658.

Tang CN, Presser F, Morad M (1988) Amiloride selectively blocks the low threshold (T) calcium channel current. Science 240:213–215.

White G, Lovinger DM, Weight FF (1989) Transient low threshold Ca^{2+} current triggers burst firing through an afterdepolarizing potential in an adult mammalian neuron. Proc Natl Acad Sci USA 86:6802–6806.

Zar JH (1984) Biostatistical analysis. Englewood Cliffs, NJ: Prentice-Hall.